International Journal of Biological Macromolecules 104 (2017) 862–873

Contents lists available at ScienceDirect

International Journal of Biological Macromolecules

journal homepage: www.elsevier.com/locate/ijbiomac

Novel oleyl amine-modified polymannuronic acid micelle loading tacrolimus for therapy of allergic conjunctivitis

Mengyi Cong[a,b,1], Zhongyu Wu[c,d,1], Xuelian Xu[a], Jiaqi Yin[a], Hongxia Li[a], Bo Zhuang[a], Cheng Wang[a,*], Xia Zhao[a,b,*]

[a] Key Laboratory of Marine Drugs, Chinese Ministry of Education, School of Medicine and Pharmacy, Ocean University of China, Qingdao, 266003, China
[b] Laboratory for Marine Drugs and Bioproducts of Qingdao National Laboratory for Marine Science and Technology, Qingdao 266237, China
[c] Institute of Materia Medica, Shandong Academy of Medical Sciences, Jinan Shandong, 250062, China
[d] School of Medicine and Life Sciences, Shandong Academy of Medical Sciences, University of Jinan, JinanShandong, 250062, China

ARTICLE INFO

Article history:
Received 18 October 2016
Received in revised form
29 December 2016
Accepted 13 June 2017
Available online 24 June 2017

Keywords:
Polymannuronic acid
Marine polysaccharide
Tacrolimus
Allergic conjunctivitis

ABSTRACT

Marine polysaccharide-based nanomaterial attracted considerable attention due to its biocompatibility and biodegradability. Here, a novel polymannuronic acid derivative (PM-C_{18}) was synthesized as nanocarrier modified with hydrophobic oleyl amine. Its structure was confirmed by Fourier-transformed infrared spectrometry and nuclear magnetic resonance. To investigate its function, we developed tacrolimus (FK506) loaded nanoparticle by self-assembling PM-C_{18} and studied its drug loading, cytotoxicity and mechanism of in vitro release. Furthermore, we established a mouse model of allergic conjunctivitis (AC) to evaluate the efficacy of FK506 loaded PM-C_{18}. The results indicated that PM-C_{18} carrier can encapsule FK506 with high drug loading (18%) and average particle size of 110.34 ± 1.6 nm. The release mechanism was diffusion initially followed a lasting release induced by swelling and collapse of PM-C_{18}. One-week treatment with FK506 loaded PM-C_{18} efficiently relieved the symptoms of AC, which indicated it could serve as a potential ophthalmic drug for patients with AC. Compared with FK506 ophthalmic suspension, FK506 loaded PM-C_{18} improved medication adherence. Most importantly, we developed a novel versatile nanomaterial of PM-C_{18} which could encapsule other active agents for more applications.

© 2017 Elsevier B.V. All rights reserved.

1. Introduction

Recently, marine polysaccharide-based nanomaterial as a novel natural source of nano-biotechnological applications have been developed extensively [1]. Due to its important properties including abundance, low cost, non-toxicity, biocompatibility and biodegradability, marine polysaccharide-based nanomaterials have received considerable attention [2]. Marine polysaccharides could be easily processed into nano-particles or micro-particles to form micelles and gels or micro-emulsions and beads, and these forms have various uses [3]. Despite using in the field of tissue engineering and wound dressing, marine polysaccharide-based nano-materials are also used as carriers to delivery materials [4]. As delivery systems, marine polysaccharides have been exactly modified to be amphipathic polymeric nano-materials. Driven by thermodynamics, polymeric materials could form micelles by self-assembly due to its amphipathy [5]. Usually, micelles have hydrophobic cores and hydrophilic shells shaped spherical in aqueous solution, the core-shell structure could serve as nano-carriers for lipophilic drugs or other biomolecules.

Taking advantages of its nanosize and surface properties, micelles are used as antitumor drug carriers a lot for tumor targeting by a passive targeting mechanism called the enhanced permeability and retention (EPR) effect [6–8], as nonviral delivery systems for plasmid DNA to achieve sustained antigen release [9], and as co-delivery systems for multiple drugs combinational therapy to overcome the drug acquired resistance [10]. Furthermore, the nanosized polymeric micelles can provide ophthalmic drug higher corneal permeability and uptake, the hydrophilic polysaccharide can reduce the irritation to epithelial cells and prolong its residence time in conjunctiva for better bioavailability [11,12].

Studies about marine polysaccharide alginate have been reported widely due to its excellent biomedical features. Alginate when less than 50 kDa could be excreted by kidneys from the body which shows its great biodegradability [13]. Alginate (Fig. 1) is a kind of marine polysaccharide consisted of two hexuronic acid

* Corresponding authors.
E-mail addresses:
cheng13980029671@163.com (C. Wang), zhaoxia@ouc.edu.cn (X. Zhao)
[1] These authors contributed equally to this work.

http://dx.doi.org/10.1016/j.ijbiomac.2017.06.064
0141-8130/© 2017 Elsevier B.V. All rights reserved.

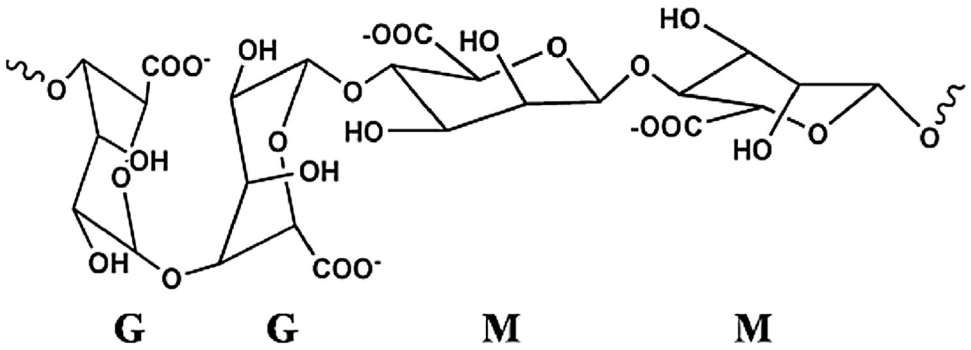


Fig. 1. Chemical structure of alginate.

residues including mannuronic acid (M) and guluronic acid (G) residues [14]. Usually, the guluronic acid (G) residues have chelating ability which could be easily cross-linked by calcium ions and other divalent cations. While the chemical modifications like esterification and acylation are merely performed on the mannuronic acid residues [15]. In this study, polymannuronic acid (PM) as the hydrophilic block is reacted with the hydrophobic long alkyl oleyl amine to get an amphipathic polysaccharide material marked as PM-C_{18}, which eventually formed polysaccharide micelle through self-assembling. The physicochemical properties including morphology, particle size, pH and cytotoxicity were tested. The sperical shape, nano-size, pH, non-toxicity and biocompatibility of PM-C_{18} make it a good drug carrier. Poorly soluble drug tacrolimus (FK506) as a drug model can be effectively incorporated into it. FK506 is a macrolide antibiotic. Due to its immunosuppressive effect, it is used for prophylaxis of organ rejection and many other immunological disorders including atopic dermatitis, ulcerative colitis and allergic conjunctivitis [16–19].

Allergic conjunctivitis (AC) is an ocular surface disease induced by abnormal and altered immunological reaction [19]. The patient with ocular surface allergy experiences extreme discomfort like itching, tearing, photophobia and sustains damage to the ocular surface, lid and conjunctiva [20]. FK506 is expected to exhibit excellent therapeutic efficacy in suppressing the abnormal immune responses of allergic ocular diseases with its immunosuppressive effect [21,22]. Here, FK506 loaded PM-C_{18} was prepared to prolong its residence time which is marked as FK506-PM-C_{18}. A mouse model of AC was established to evaluate its therapeutic effect. The treatment results showed FK506-PM-C_{18} could relieve the symptoms of AC efficiently. Compared to free FK506 ophthalmic suspension, it could improve the treatment compliance of AC. Finally, the novel nanomaterial of PM-C_{18} we synthesized could encapsule other active agents for more applications.

2. Materials and methods

2.1. Materials, cell lines and animals

Polymannuronic acid (PM) was obtained from Key Laboratory of Glycoscience and Glycotechnology of Shandong Province (China), The weight average molar mass of PM is 9200 Da measured by Size Exclusion Chromatography (SEC Agilent-1260 USA) with Tsk-G3000 column (300 × 7.8 mm, 5 μm) purchased from Zhongran Technology Company (Huai'an, China), Tacrolimus (FK506) was from Zhengzhou HuaYao biological technology co., Ltd. (Zhengzhou, China), 1-(3-dimethylaminopropyl)-3-ethylcarbodiimide hydrochloride (EDC), N-hydroxysuccinimide (NHS) and 0.25% (w/v) trypsin–0.1% (w/v) Ethylene Diamine Tetraacetic Acid (EDTA) were purchased from Solarbio (Beijing Solarbio Science and Technology, China). Oleyl amine ($C_{18}H_{37}N$, A.R.), Dimethyl Formamide (DMF, A.R), Aluminum hydroxide (Alum, A.R), Chloroform (A.R), Ethanol absolute (A.R) and spectrographic grade potassium bromide (KBr) were obtained from Sinopharm Chemical Reagent Co., Ltd. (Shanghai, China). HPLC-grade acetonitrile was purchased from Anaqua Chemical Supply (Houston, TX, USA). Dulbecco's Modified Eagle Medium (DMEM) High Glucose was purchased from HyClone Thermo Scientific. Fetal Bovine Serum (FBS) was from Gibco-Life Technologies. Dimethylsulfoxide (DMSO), ovalbumin (OVA)and 3-(4, 5-dimethylthiazol-2-yl)-2, 5-diphenyl-tetrazolium bromide (MTT) were from Sigma (Sigma-Aldrich Corp.USA). Culture flasks and dishes were from Corning (Corning, NY, USA). All other chemicals were of analytical reagent grade and purchased from commercial sources.

Mouse fibroblast cell line L929 was purchased from the Type Culture Collection of the Chinese Academy of Sciences (Shanghai, China). The cells were cultured in DMEM medium, together with 10% FBS and 1% penicillin-streptomycin, at 37 °C in a humidified incubator in 5% CO_2.

Female Kunming (KM) mice (6–8 weeks, 18–20 g, n = 20) were purchased from the Institute for Drug Control of Qingdao. Adequate food and water were provided for the animals. They were kept at temperature of 20–22 °C, relative humidity of 50–60% and 12 h light-dark cycles. All animal treatments and experiments were carried out according to Institutional Animal Care and Use guidelines. The animal experiments were approved by Ethics and Animal Welfare Committee of School of Medicine and Pharmacy, Ocean University of China.

2.2. Synthesis of hydrophobic polymannuronic acid (PM-C_{18})

The synthesis method of PM-C_{18} is derived from the procedure previously described [14]. The synthetic route is showed in Fig. 2. Briefly, PM was first dissolved into distilled water and changed pH to 5.5 with phosphate buffer solution. Then EDC and NHS were added to the solution to activate the carboxyl groups of PM for 10 min. The molar ratio for PM (with reference to the carboxyl groups), EDC and NHS was 2:2:1 to make sure the catalysts could catalyze efficiently. At the same time, oleyl amine was dissolved into organic solution consisted of DMF and Ethanol absolute (V/V = 1:1). Later oleyl amine together with DMF and ethanol absolute were dropped into the PM solution mentioned above slowly. The mixed solution was continuously stirred for 24 h at room temperature. After the reaction finished, a great quantity of ethanol absolute was added to precipitate the polymer produced and the precipitate was washed with ethanol absolute several times. Then the precipitate was dissolved into distilled water and dialyzed using dialysis tubes with cutting off molecular weight of 14000 for at least 3 days using distillated water which was replaced daily, finally it was concentrated with vacuum rotary evaporator (Laborota 4000; Heidolph Instruments GmbH & Co., KG, Germany) and lyophilized

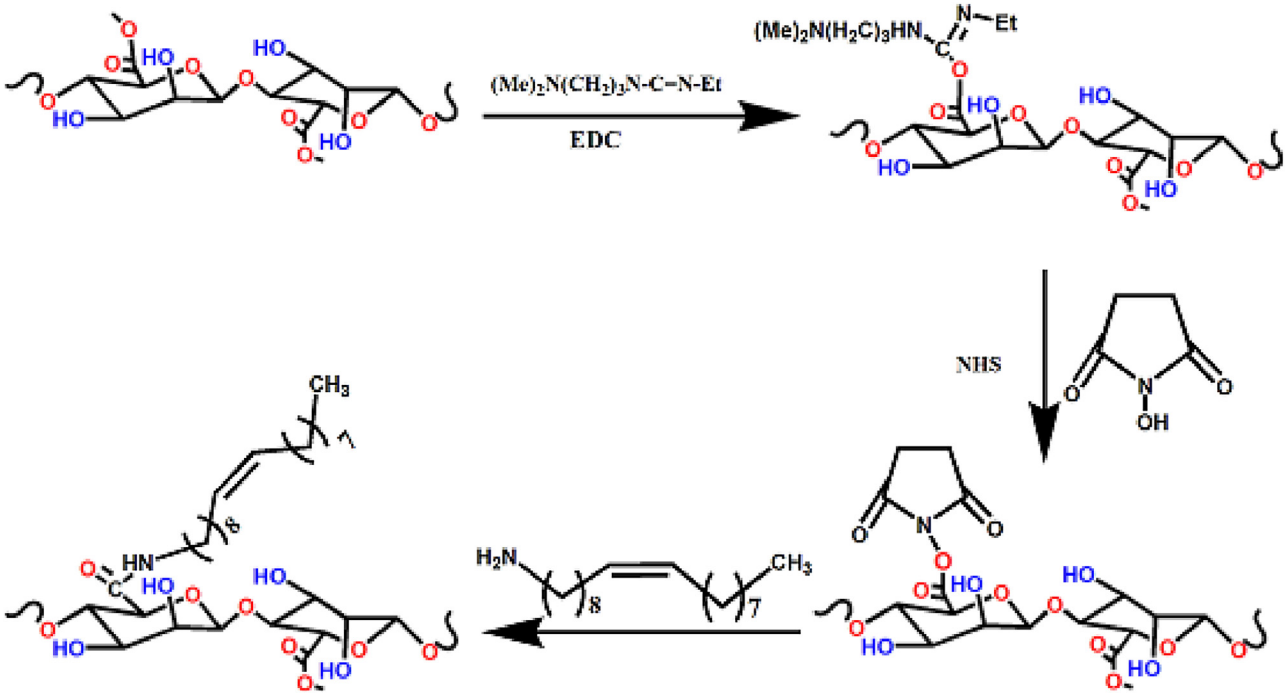


Fig. 2. The synthetic route of PM-C_{18}.

using freeze drier (FD-1C-50, Boyikang Instrument Co., Ltd., China). The product was marked as PM-C_{18}.

2.3. Characterization of PM-C_{18}

Infrared spectrum measurement was carried out on a FTIR Analyzer (Nexus 470 by Nicolet Instruments America). A total of 2% (w/w) of the sample was dispersed in KBr and then compressed to tablets. Each tablet was scanned between 400 and 4000 cm^{-1}. ^1H NMR was performed on a nuclear magnetic resonance spectrometer (JNM-ECP600, JEOL TMS, Tokyo, Japan) at 25 °C. The sample was dissolved in D_2O to a concentration of approximately 10 mg/mL.

2.4. Preparation of blank PM-C_{18} micelle

PM-C_{18} micelle was prepared by self-assembly method [23]. Briefly, PM-C_{18} copolymer was directly added in water followed by Ultrasonic dissolution. When the temperature was up to 50 °C, due to the amphiphilic properties, the PM-C_{18} copolymer self-assembled into micelles triggered by temperature increasing. Few minutes later, the micelle solution was cooled to room temperature. The product was the PM-C_{18} micelle.

2.5. Characterizations of the PM-C_{18} micelle

2.5.1. The physical properties

The mean diameter and polydispersity index (PDI) were analyzed by dynamic light scattering (DLS) using Malvern nano-S90 particle size analyzer (Malvern, Worcestershire, UK).The samples were diluted with ultra-filtrate distilled water to form suspension with a concentration of 1 mg/mL. Then they were placed in vertical cylindrical cells (10 mm-diameters) and measured for at least three repetitions.

The morphology of micelle was observed by negative staining method [24]. Briefly, a drop of the nanoparticle suspension (1 mg/mL) was placed on formvar-coated copper grid (Taab Labs Ltd., England) and stained with 2% phosphotungstic acid. After air-dried at room temperature, they were measured with transmission electron microscopy (JEOL JEM-1200EX, Ltd., Japan).

The pH of the PM-C_{18} micelle (1.5 mg/mL) was investigated by pH meter (Starter 2100, Ohaus, USA) and the measurement was repeated three times.

2.5.2. in vitro cytotoxicity evaluation

Cytotoxic activity of PM-C_{18} was performed on mouse fibroblast cell line L929. After harvested by treating with 0.25% (w/v) trypsin–0.1% (w/v) EDTA solution, L929 cells in DMEM completed medium (200 μL) were seeded in a 96-well plate (8×10^3 cells/well). After 24 h incubation, they were exposed to 0, 200, 500, 1000, 1500, 2000 μg/mL PM-C_{18} micelle solution for 72 h respectively [25]. Cell viability was measured using MTT method [26]. Briefly, MTT solution (5 mg/mL, 20 μL/well) was added and aspirated off gently after incubation for 4 h. DMSO (150 μL/well) was then added to dissolve the crystals and the absorbance of it was measured at 490 nm by a microplate reader (SPECTRA-max M5, Molecular Devices, USA). The relative cell viability (%) was applying with (Abs sample/Abs control) × 100%. Here, cells exposed to 0 μg/mL PM-C_{18} micelle solution were taken as control with 100% viability. The results were expressed as mean values ± SD of five measurements.

2.6. Preparation and characterization of FK506 loaded PM-C_{18} micelle

FK506 loaded PM-C_{18} micelle was prepared by o/w emulsion method as previously reported [27,28]. In brief, 2 mL chloroform with different amount of FK506 was added to 10 mL aqueous PM-C_{18} micelle solution (1 mg/mL), then ultrasonic emulsificated by Ultrasonic Cell Crusher (VCXl05, Sonics, USA), forming the o/w emulsion. The organic solvent chloroform in the emulsion was removed by using vacuum rotary evaporator (Laborota 4000, Heidolph Instruments GmbH & Co., KG, Germany). The solutions were then filtered through 0.45 μ m syringe filter (Millex-LG, Millipore Co., 109 USA) to remove unloaded FK506. Finally, the drug loaded

micelles were lyophilized using the freeze drier. The products were marked as FK506-PM-C_{18}.

The mean diameter, polydispersity index (PDI) and the morphology of the FK506-PM-C_{18} were measured according to the method mentioned above. Moreover, atomic force microscopy (AFM) (Agilent Technologies, Inc., 5400 AFM/SPM) was utilized to obtain the 3D images of the sample [29]. In brief, a droplet of suspension (1 mg/mL) was put on the polyethylene imine coated glass cover slip and air dried. By scanning with the probe tip, sample was then imaged with Nano-scope III (Digital Instrument/VEECO).

In order to identify FK506 was loaded in PM-C_{18}, FTIR spectroscopy of PM-C_{18}, FK506, FK506-PM-C_{18} and physical mixture of PM-C_{18} and FK506 were measured as introduced above.

2.7. Drug loading and encapsulation efficiency of FK506-PM-C_{18}

Drug loading (DL) and encapsulation efficiency (EE) of the FK506-PM-C_{18} were determined as follows. Lyophilized powder FK506-PM-C_{18} was dissolved in acetonitrile to destroy the structure of micelle. After filtered by 0.22 μm syringe filter (Tianjin Jinteng Experiment Equipment Co., Ltd, Tianjin, China), the content of FK506 was determined by high performance liquid chromatography (HPLC). The DL and EE were calculated according to Eq. (1) and Eq. (2):

$$DL\% = \frac{FK506}{(Copolymer + FK506)} \times 100\% \quad (1)$$

$$EE\% = \frac{\text{Weight of FK506 in micelle}}{\text{Weight of feeding FK506}} \times 100\% \quad (2)$$

The concentration of FK506 was determined by HPLC 1260 infinity system equipped with a VWD detector (Agilent, Sunnyvale, CA, USA). The chromatographic analysis was performed on a Hypersil BDS C18 (150 mm × 4.6 mm, 5 μm, Dalian Elite Analytic Instruments Co., Ltd, Dalian, China), using 90% acetonitrile and 10% water as mobile phase at a flow rate of 1.0 mL/min. The column temperature was kept at 50 °C and FK506 was monitored at the wavelength of 225 nm [30]. The standard curve equation is: A = 6.512*C + 2.917 (A: The area of peak; C: The concentration of FK506) and the correlation coefficient is 0.9997.

2.8. in vitro drug release

A modified dialysis method was used to determine the release behavior of FK506-PM-C_{18} in vitro [31]. Briefly, free FK506 dissolved in acetonitile and FK506-PM-C_{18} dispersed in distilled water were placed in dialysis bags (molecular mass cutoff is 3.5 kDa). The dialysis bags were incubated in 15 mL of pre-warmed phosphate buffered saline (PBS, 37 °C, pH 7.4) containing Tween 80 (0.5%, w/v) with horizontal shaking (100 rpm) at 37 °C. At specific time intervals, 1 mL release medium was removed and filtered through 0.22 μ m syringe filter (Millex-LG, Millipore Co., 109 USA), the rest of release medium was removed and replaced by pre-warmed fresh medium. Concentration of FK506 was quantified using HPLC with the same method above-mentioned. All results were the mean of three samples, and all data were expressed as the mean ± SD.

2.9. Induction and treatment of allergic conjunctivitis (AC)

KM mice were raised on the laboratory standard for one week. Afterwards, the model of AC was established as described earlier [32,33]. As shown in Fig. 7A, mice except the normal group (n = 5) were sensitized intraperitoneally (i.p.) with immunization which consists of 100 μg of OVA and 1 mg of aluminum hydroxide (Alum) thoroughly mixed in 200 μL of PBS (pH 7.4) on day 1, 8, 15, then challenged by instillation of OVA eye drops (200 μg/5 μL) daily for seven days.

In order to verify the FK506-PM-C_{18} formulation could reduce the eye instillation times, improve treatment compliance and increase the drug bioavailability. After the AC models were established, they were randomly divided into three groups (n = 5/group), named control, FK506 and FK506-PM-C_{18}. 5 μL drop of normal saline, 0.03% FK506 (dissolved with 0.3% hydroxypropyl methylcellulose normal saline) and 1.5 mg/mL FK506-PM-C_{18} solution were instilled to each group. The FK506-PM-C_{18} group was instilled twice a day and other two groups three times a day. The treatment lasted for seven days.

3. Slit lamp evaluation

To monitor the progression of treatment, ocular surface evaluation was assessed at 4 time points 20 min after allergen challenge during the treatment period. Each un-anesthetized mouse was assessed and photographed by a slit lamp (TOPCON, BGIUNIT BG-4) under natural light and a macrolens in blinded fashion. A score system was used to grade the degree of the AC [34]. Conjunctival edema, conjunctival redness, lid swelling, and mucus secretion were each graded on a 0–4 according to the severity (Table 1). The slit lamp evaluation score was the sum of the four parameters, thus the score represented the degree of the AC. To avoid observer variability, there was only one masked reader for all mice.

3.1. Histological analysis

The entire eyes were enucleated with the lids in all groups and immediately fixed in 10% buffered formalin. After dehydration, the tissues were embedded in paraffin. 3-μm thickness sections were dewaxed by immersion in xylene (3 times for 5 min each time) and hydrated with different concentrations of alcohol and stained with hematoxylin-eosin. The inflammatory cells in conjunctival epithelium and subepithelium were evaluated under the same microscope field with a microscope (OLYMPUS BX60, Japan) and imaging analyzing system (OLYMPUS DP25, Japan). Because the number of inflammatory cell was not always uniform throughout the sections, three different sections were selected for counting, and an average was calculated [35]. Three mice were evaluated in each treatment group.

4. Statistical analysis

Data were expressed as the mean value ± SD. The number of inflammatory cells from each group of mice was carried out using with one-way analysis of variance (ANOVA) using SPSS 17.0 software (SPSS Inc., Chicago, IL). A P value < 0.05 was considered statistically significant.

5. Results and discussions

5.1. Characterization of PM-C_{18}

5.1.1. FTIR analysis

The FTIR spectra of the poly mannuronic acid (PM) and hydrophobic poly mannuronic acid (PM-C_{18}) are shown in Fig. 3. There is a wide peak at 3434 cm^{-1} indicating O—H stretching vibrations in both spectras. The presence of two bands at 1607 and 1450 cm^{-1} are due to the existence of carboxylic acid groups. These peaks are also present in PM-C_{18} spectra, however, the change in the size of the peaks is accompanied by appearance of new little peak at 1735 cm^{-1}, indicating the change of some carboxylic acid groups of PM. Additionally, the new peaks at 2854 and 2920 cm^{-1}

Table 1
Slit lamp evaluation of AC.

Evaluation signs	None 0	Minimal 1+	Mild 2+	Moderate 3+	Severe 4+
Lid swelling	Absent	Minimal	Focal areas	Obvious	Severe
Conjunctival redness	Normal	Pink	Red	Diffuse red	Dark red
Conjunctival edema	Normal	Minimal	Focal areas	Diffuse edema	Severe
Mucus secretion	No discharge	Filaments of Mucus	Moist lids and hair	Moist lids, hair and mucus	Severe mucus secretion

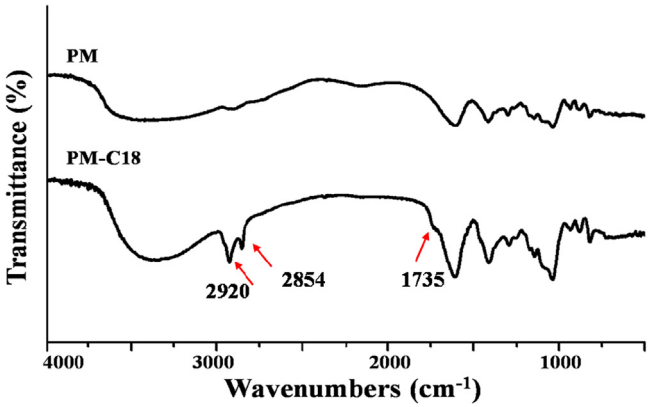


Fig. 3. Fourier transforms infrared spectra of the PM and PM-C_{18} (red arrow: new peaks). (For interpretation of the references to colour in this figure legend, the reader is referred to the web version of this article.)

represent the stretching vibrations of alkyl groups of oleyl amine which also predicating there are long alkyl groups on PM-C_{18}. All these phenomenons could suggest the amide reaction took place [15]. When alginate was modified by octyl amine in previous paper, peaks of methylene groups at 2924 and 2825 cm^{-1} appeared and the band of the wide peak at 3434 cm^{-1} was also sharper after the amidation [36].

5.1.2. ^1H NMR analysis

The structure of PM-C_{18} was further confirmed by ^1H NMR. As shown in Fig. 4, the chemical shift of 0.7 ppm is attributed to the protons of the methyl with the integral of 1.00 marked as $\int$ a. Due to the influence of water, the anomeric proton of the polymannuronic acid around 4.6 ppm could not be seen clearly, while the other protons with chemical shift around 4.0-3.2 ppm could be integrared as 5.43 marked as $\int$ b. The grafting yield is the ratio of number of $C_{18}H_{37}N$ (Nc) and the number of PM (Np). Through the integrals of the ^1H NMR spectra, we know $\int$ a/3Nc is equal to $\int$ b/4 Np. The grafting yield could be calculated from the following formulae:

$$\text{Grafting yield\%} = \frac{\text{Nc}}{\text{Np}} \times 100\% = \frac{4\int a}{3\int b} \times 100\% = 24.6\%$$

5.2. Characterization of PM-C_{18} micelle

5.2.1. Particle size, morphology and pH

DLS analysis is a common way to characterize the size dispersion and aggregation process of micelle. The size of micelle affects their biological characteristics like physical, chemical, pharmacokinetics, electromagnetic activities and behaviors when used as drug delivery and tumor targeting materials. What's more, the shape and size could prevent the nanoparticles from premature blood clearance by the reticuloendothelial system (RES) [37] and can increase blood circulations which enable the accumulation of the particles in tumors by the enhanced permeability and retention (EPR) effect [38]. The particle size of octanol–grafted alginate nanoparticles in other study was 180.6 ± 1.2 nm [15]. The particle size distribution for the PM-C_{18} micelle is represented in Fig. 5C, which shows the

Table 2
The DL, EE, Particle Size and PDI of FK506-PM-C_{18} micelles.

FK506 (mg)	DL (w/w%)	EE (%)	Size (nm)	PDI
1.54	14.53 ± 0.14	96.87 ± 0.76	115.89 ± 2.10	0.187 ± 0.053
2.02	16.83 ± 0.07	95.57 ± 0.48	126.62± 1.34	0.166 ± 0.017
2.53	18.67 ± 0.03	90.57 ± 0.78	139.64 ± 1.68	0.211 ± 0.042

average particle size is 110.34 ± 1.6 nm (PDI = 0.236 ± 0.01). Particles ranged 100–200 nm can be internalized by receptor-mediate endocytosis, while larger particles have to be taken up by phagocytosis [39]. When particles shape with a size range around 100 nm, they have been shown to have higher cellular and tissue uptake [40].

The TEM (Fig. 5A) image reveals that the morphology of PM-C_{18} is spherical and homogeneous. From the image, the particle sizes are about 50 nm with a narrow particle size range. The TEM determines the size of dry particles while the DLS determines the hydrodynamic diameter of particles in water. The size determined by DLS is always larger than that determined by TEM because of the loose structure of amphiphilic micelles in water. The diameter observed by TEM is in good agreement with the results of particle size analysis.

The pH of eye drop formulation is correlated to the irritation and the pH range of 6–8 has no irritation to eyes. The pH of PM-C_{18} micelle (1.5 mg/mL) is found to be 6.21 ± 0.28, which is a little lower than the pH of tears. The tears have a wide buffering capacity, so no pH adjustment was made here.

5.2.2. Cytotoxicity evaluation

The cytotoxicity of PM-C_{18} on L929 cells was evaluated by MTT assay. As Fig. 5B presented, viability of L929 cells decreased with increasing the concentration of PM-C_{18}. The cell viabilities are still above 85%, even the concentration of the copolymer is up to 2000 μg/mL for 72 h. These results indicate that PM-C_{18} is biocompatible with noncytotoxicity and could serve as a drug carrier.

5.3. Characterization of FK506-PM-C_{18} micelle

The appearances of distilled water, PM-C_{18} and FK506-PM-C_{18} solution are shown as Fig. 6A. The translucent blue opalescent appearance of redissolved PM-C_{18} and FK506-PM-C_{18} reveals that the micelles are homogeneous, stable and can be well dispersed in aqueous solution. Furthermore, the translucent blue opalescent appearance of FK506-PM-C_{18} micelle is more obvious than that of PM-C_{18} counterpart, which means the loading of FK506 make the diameter of micelle larger. DLS, TEM and AFM are also used here to reveal the size and morphology of the FK506-PM-$C_{18,}$ compared to PM-$C_{18,}$ drug loaded micelles have larger sizes shown in Fig. 6D and Table 2. From the TEM and AFM image, the spherical and homogeneous drug loaded micelle image can be seen clearly in Fig. 6B, C.

To examine encapsulation of FK506 in PM-C_{18}, FTIR measurement was performed on PM-$C_{18,}$ FK506, FK506-PM-C_{18} and the physical mixture of PM-C_{18} and FK506. As Fig. 6E shows, in the spectrum for FK506, the peaks at about 3663 cm^{-1} and 1741 cm^{-1} are assigned to be the typical peaks of FK506, these peaks disappear in FK506-PM-C_{18}, but still exist in the physical mixture, indicat-

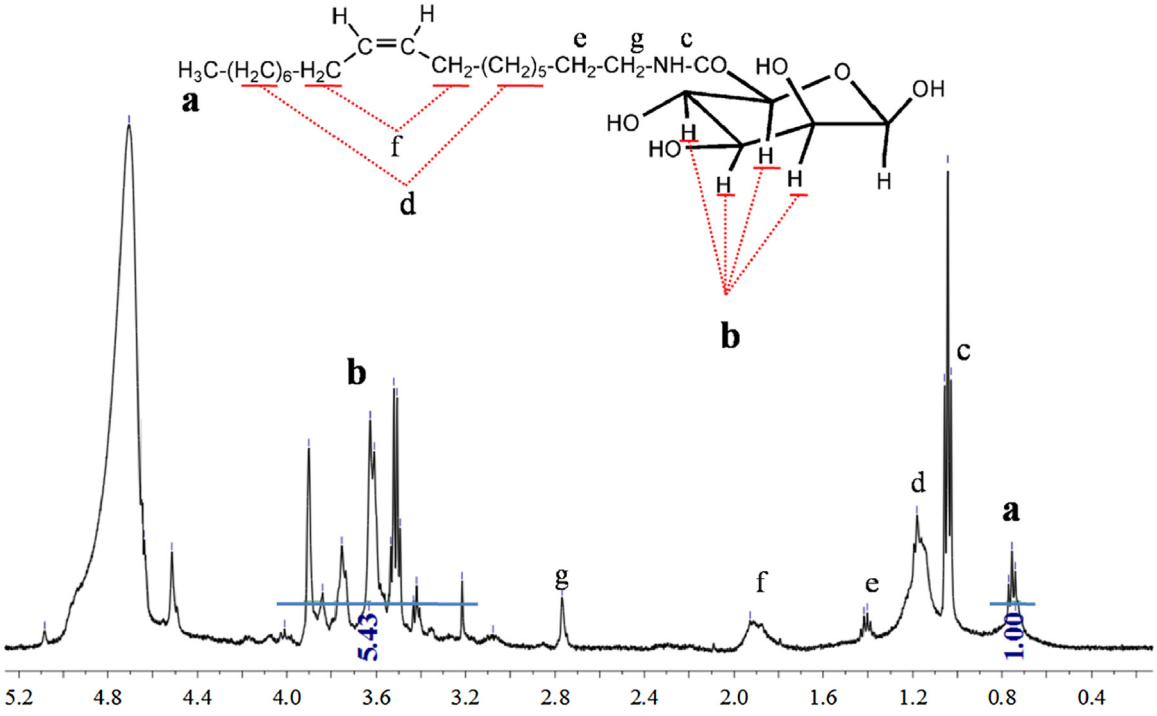


Fig. 4. The ^{1}H NMR spectrum of PM-C_{18}.

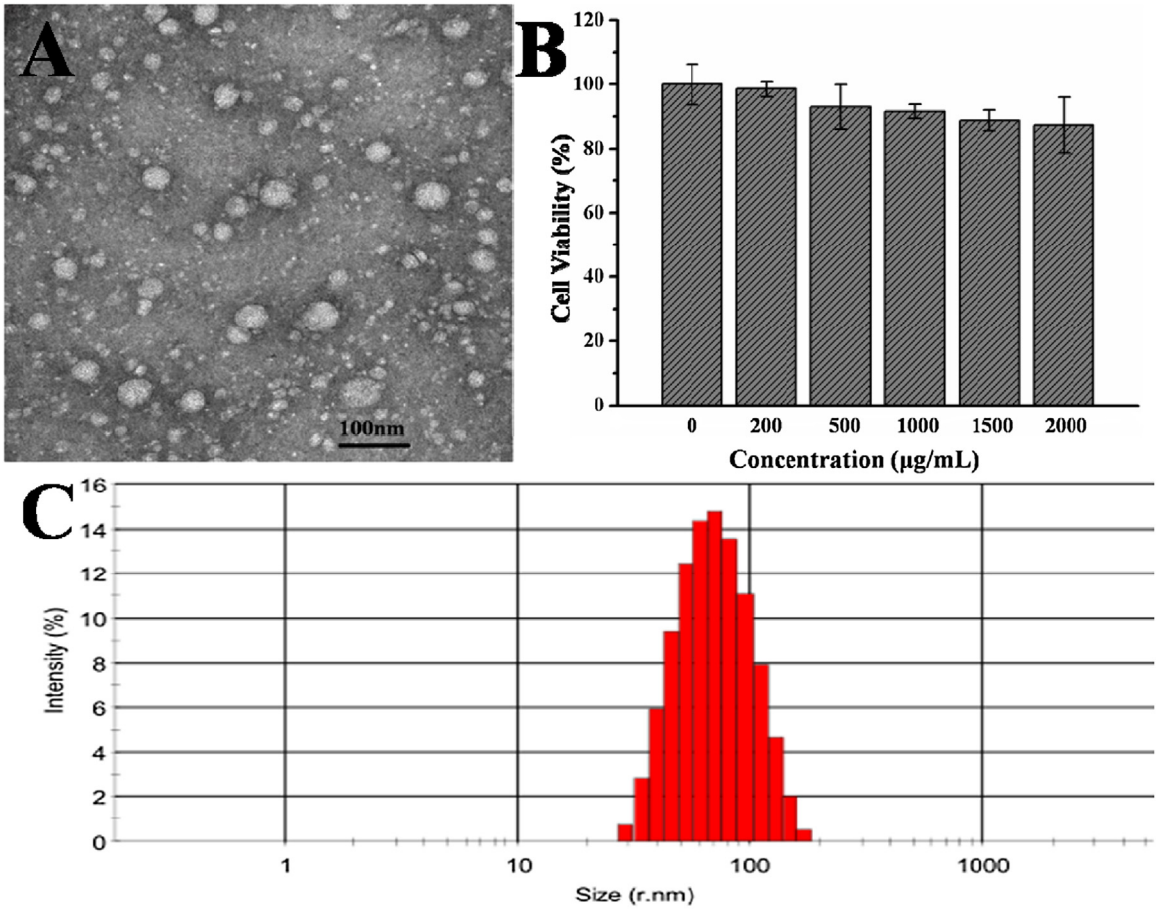


Fig. 5. Characterization of Blank PM-C_{18}. (A) TEM image of PM-C_{18} and the scale bar is 100 nm. (B) Cytotoxicity of PM-C_{18} at different concentration on L929 cells 72 h. (C) Particle size distribution of PM-C_{18o}.

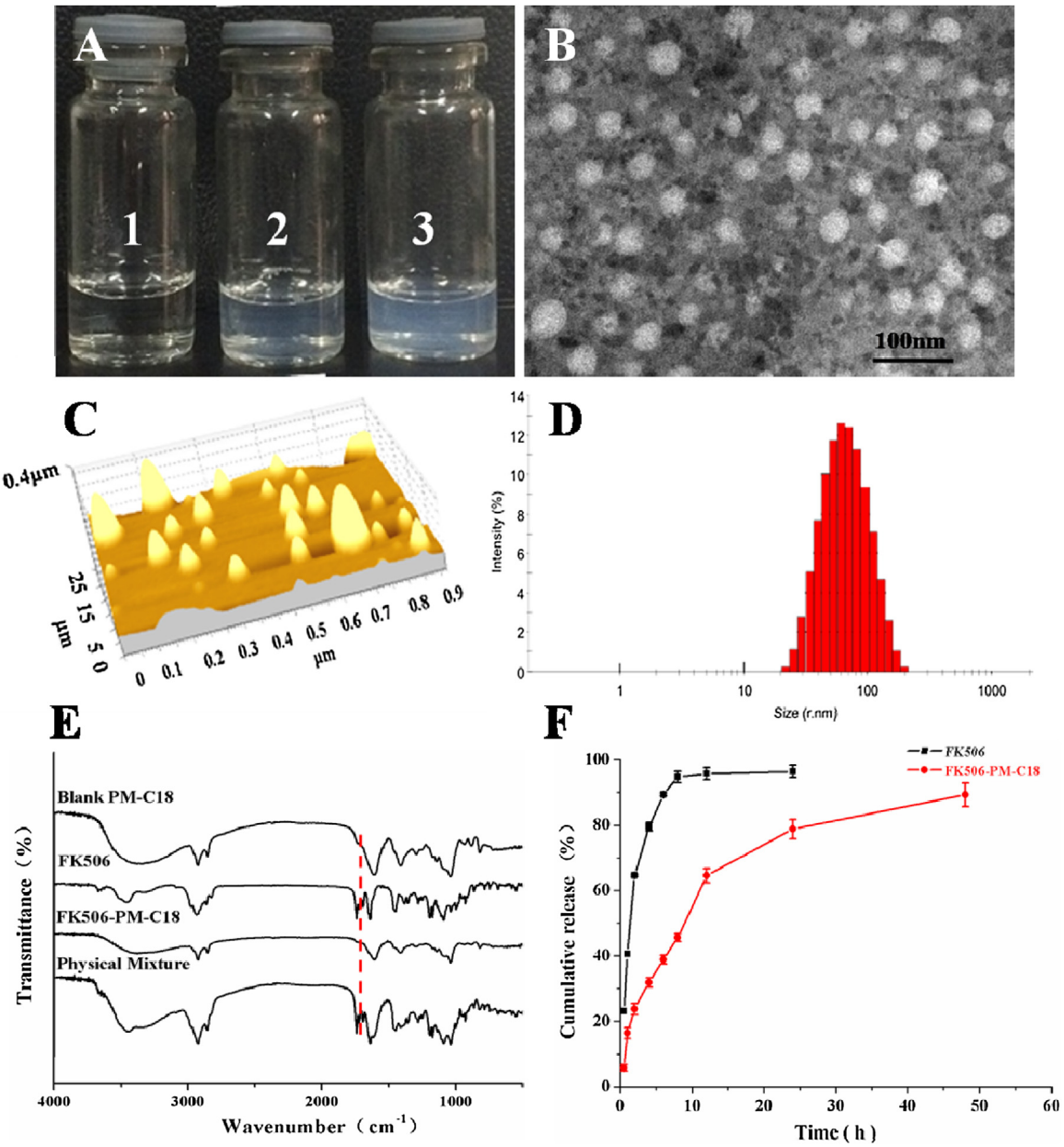


Fig. 6. Characterization of FK506-PM-C_{18} (DL = 18%). (A) The appearance of distilled water (1), redissolved PM-C_{18} solution (2), redissolved FK506-PM-C_{18} solution (3). (B) TEM image of FK506-PM-C_{18} and the scale bar is 100 nm. (C) AFM image of FK506-PM-C_{18}. (D) Particle size distribution of FK506-PM-C_{18}. (E) FTIR spectra of blank PM-C_{18}, pure FK506, lyophilized powder of FK506-PM-C_{18}, and physical mixture of PM-C_{18} and FK506. (F) In vitro release curve of FK506 and FK506-PM-C_{18} solution. (n = 3).

ing that FK506 is molecularly incorporated in the micelles and no chemical reaction occurred.

Moreover, the results of DL and EE of FK506-PM-C_{18} were shown in Table 2. When the DL increased from about 14.53% to 18.67%, the EE decreased from 96.87% to 90.57% and the particle size increased from 115.89 nm to 139.64 nm. The particle size is still in the range of endocytosis. Due to its high DL and relatively good EE, we choose the DL 18.67% for following study.

5.4. *in vitro drug release behavior*

The in vitro release behaviors of FK506 and FK506-PM-C_{18} are illustrated in Fig. 6F. As we can see, compared to the rapid release profile of FK506, the release profile of FK506-PM-C_{18} is relatively gentle without a burst effect. 94.71% of FK506 is released within 8 h which demonstrates that the dialysis membrane has no blocking effect on retarding the release of the drug. The release profile of FK506-PM-C_{18} proceeds in two stages: an initial relatively rapid stage and a long-lasting release stage. The cumulative release rate during first stage is 64.53% ± 5.77% and the second stage is the long lasting release stage till the second day. Finally, the cumulative release rate is 89.25% ± 6.95%. In previous paper, FK506-loaded PLGA and PLA microspheres with higher DL (up to 31%) could release for at least 2 weeks by a single intramuscular administration [16].

To evaluate the release behaviors, several drug release kinetic models (including First order, Higuchi, Baker-Lonsdale and Weibull modeling) were adopted, and the results were presented in Table 3. The release profile of the FK506 fits well to First order model (r = 0.9973) and Weibull model (r = 0.9982) while FK506-PM-C_{18} fits to Weibull model (r = 0.9954) and Baker-Lonsdale model (r = 0.9944). The Baker-Lonsdale model is developed from Higuchi

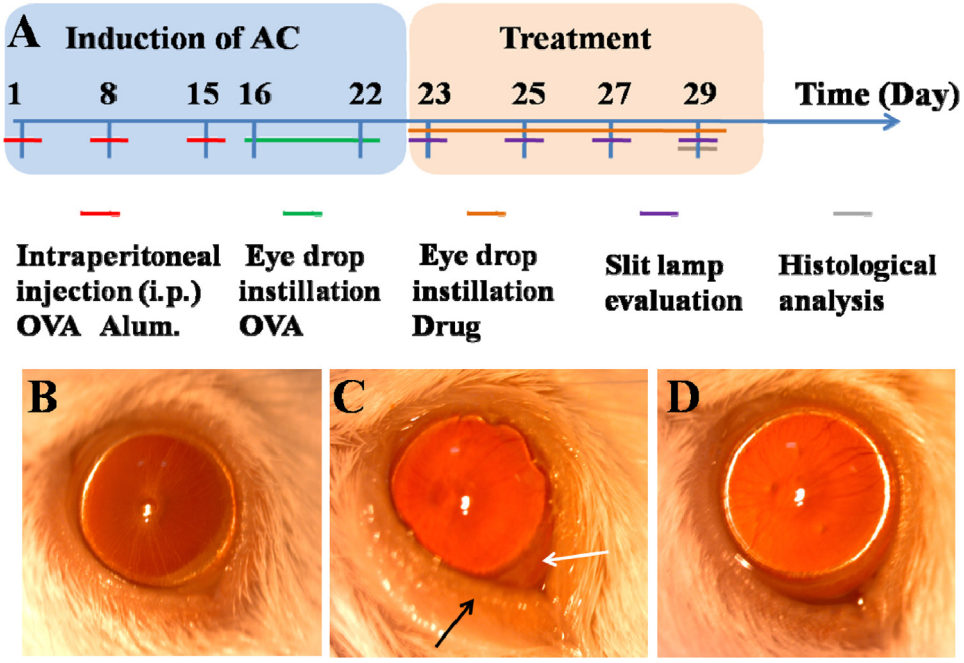


Fig. 7. (A) The experimental procedure. (B) The picture of normal eye under slit lamp. (C) The picture of eye with AC under slit lamp (black arrow: lids swelling; white arrow: conjunctival edema). (D) The picture of eye after treatment under slit lamp.

Table 3
Release kinetics of FK506 and FK506-PM-C_{18}.

Kinetics model	FK506		FK506-PM-C_{18}	
First order	Q=100*[1-Exp(-0.471*t)]	r=0.9973	Q=100*[1-Exp(-0.082*t]	r=0.9930
Higuchi	Q=33.396+16.896*tô.5	r=0.8410	Q=8.406+12.041*tô.5	r=0.9678
Baker-Lonsdale	3/2*[1-(1-Q/100)^(2/3)]-Q/100=0.02*(t+1.183)	r=0.9121	3/2*[1-(1-Q/100)^(2/3)]-Q/100=0.007*(t-0.413)	r=0.9944
Weibull	Q=96.212*{1-Exp[-(tô.899)/1.815]}	r=0.9982	Q=103.148*{1-Exp[-(tô.721)/7.045)]}	r=0.9954

model which is more suitable to describe the drug release from spherical matrices [41]. The free drug FK506 is released by passive diffusion dependent on the concentration gradient between the sample and the release media. While the drug release from FK506-PM-C_{18} should consider the interaction between the drug and the micellar kernel [35]. As expected, the release mechanism was diffusion initially followed by a lasting release induced by swelling and collapse of PM-C_{18} [42]. Considered of its release behavior, FK506-PM-C_{18} could reduce the frequency of administration.

5.5. Slit lamp evaluation scoring

Through the induction of AC, eyes exposed to OVA have several signs of AC after the allergen challenge compared to normal group (Fig. 7B). Notice presence of lid swelling, mucus secretion and conjunctival edema could be seen in Fig. 7C. After one week treatment, the symptoms of AC had relieved which could be seen in Fig. 7D.

The control group treated with normal saline had more conjunctival edema, redness and mucus secretion than the FK506 group and FK506-PM-C_{18} group (Fig. 8A). As for the FK506 group and FK506-PM-C_{18} group, no big difference was shown from the slit lamp evaluation scores (Fig. 8B), the scores of these two groups reduced from around 7 to around 3, which demonstrated FK506 had the prominent therapeutical effect and the drug carrier PM-C_{18} maintaind the drug activity. The mechanism of FK506 is based on the inhibition of the phosphatase activity of calcineurin and the activation of the dephosphorylation of the nuclear factor of T-cell protein, which is a necessary transcription factor for the expression of inflammatory cytokines. Besides, it could downregulate the expression of the high-affinity IgE receptor and inhibite the release of inflammatory mediators from mast cells [19]. The treatment of FK506 and FK506-PM-C_{18} reduced abnormal and altered immunological reaction after the allergen challenge intuitively from the ocular surface clinical evaluation.

5.6. Morphology of the conjuncitva histology

The conjunctival sac is a kind of cystic space formed by conjunctiva. The normal conjunctival epithelium shows polarity, consisting of single-layered goblet cells and one or two-layered epithelial cells [43]. (Fig. 9A) The goblet cells play an important role in preserving the health of ocular surface [44]. When the mice were inducted of AC, their conjunctival epithelium lose some goblet cells even emerged subjective complains of dry eye, besides the layers of epithelial cells may increase and show squamous metaplasia, at the same time plenty of inflammatory cells could be seen in conjunctival epithelium and subepithelium (Fig. 9B).

After one week treatment, obvious differences could be seen from the treatment groups, the goblet cells increased, the squamous metaplasia decreased and the inflammatory cells also decreased compared with the control group. As shown in Table 4, the number of inflammatory cells in subepithelium of control group was 53.6 ± 29.93, the FK506 group and the FK506-PM-C_{18} group were 11.4 ± 6.23 and 10.4 ± 10.74 respectively and the normal group was 4.0 ± 3.53. Though compared to the normal group, the treatment groups still had higher degree of inflammatory cells infiltration, both of the two groups showed much fewer of inflammatory cells in subepithelium. There was hardly any inflammatory cell in epithelium after one week treatment.

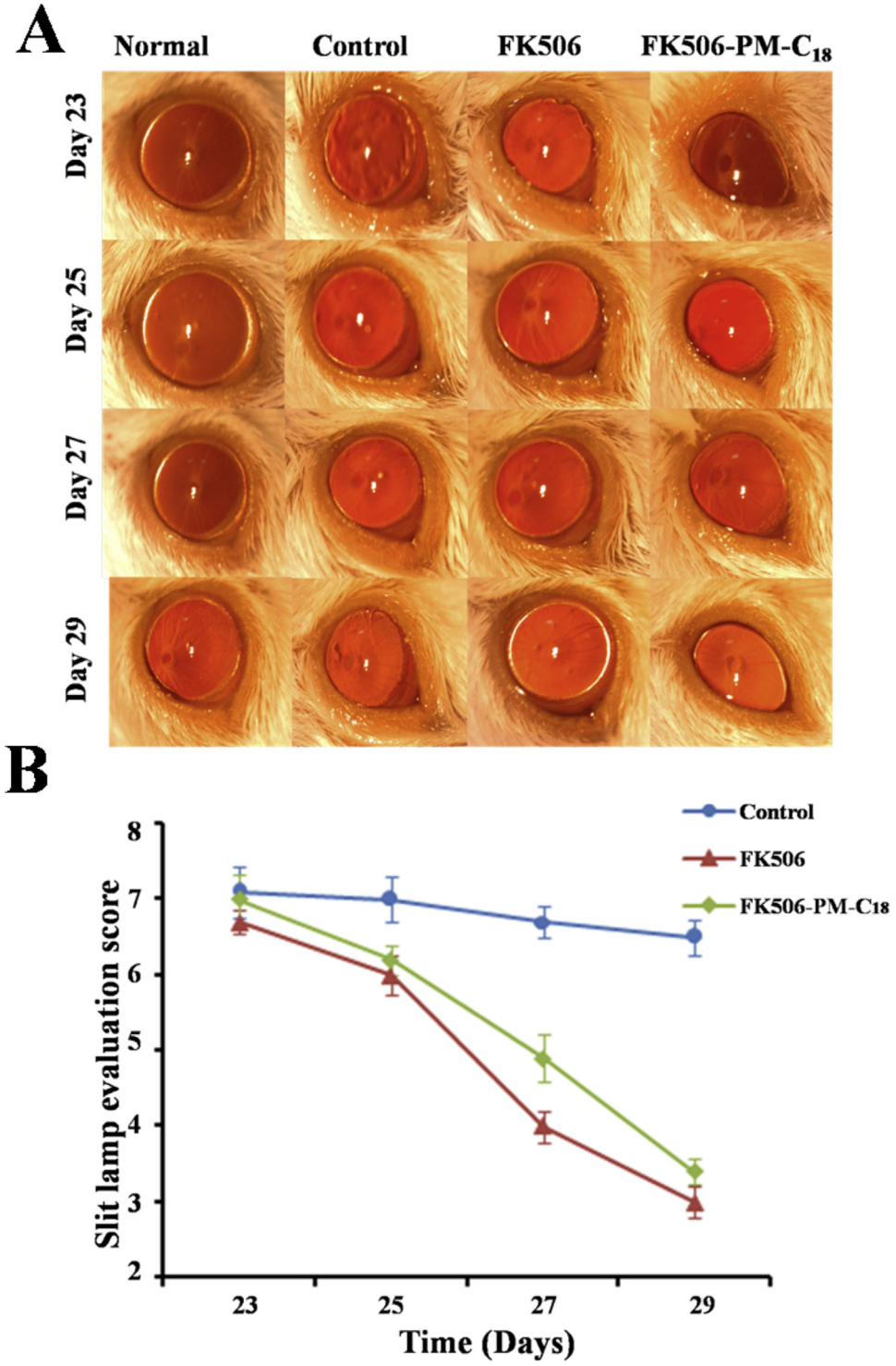


Fig. 8. (A) Pictures of eyes under a slit lamp microscope of normal, negative control, FK506, FK506-PM-C_{18}. (For interpretation of the references to color in this figure legend, the reader is referred to the web version of this article). (B) Slit lamp evaluation scores of AC during treatment. Data show mean ± SD (error bars).

Table 4
The number of inflammatory cells.

	Normal	Control	FK506	FK506-PM-C18
Inflammatory cells in epithelium	0 ± 0	4.8 ± 2.28	0.2 ± 0.45*	0 ± 0*
Inflammatory cells in subepithelium	4.0 ± 3.53	53.6 ± 29.93**	11.4 ± 6.23*	10.4 ± 10.74*

Values are expressed as means ± SD.
* P <0.05 versus control.
** P < 0.01 versus normal.

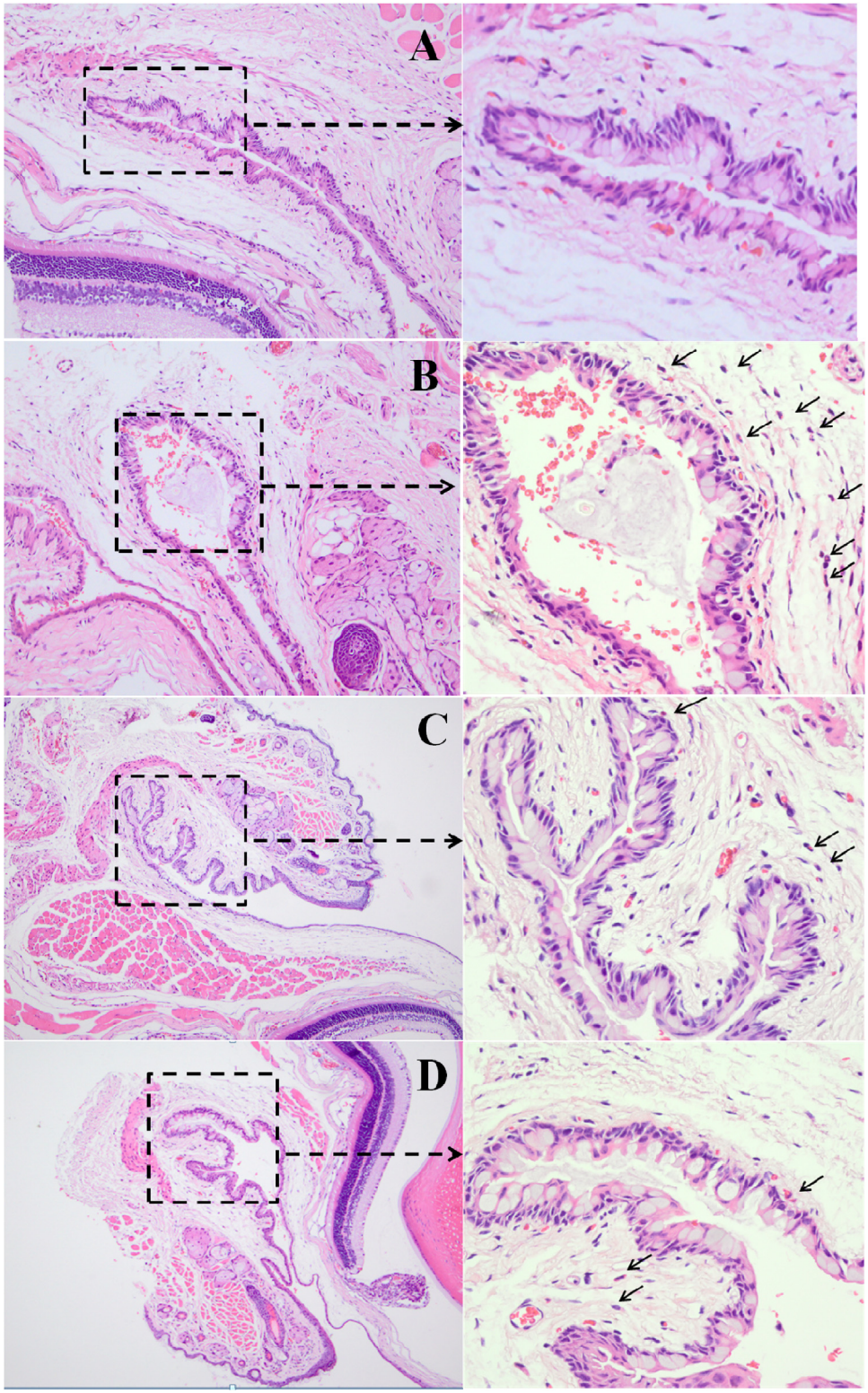


Fig. 9. Histopathologic analysis of the conjunctiva using a microscope with × 100 magnification (left) and × 400 magnification (right) at day 29. (A) normal group (B) control group (C) FK506 group (D) FK506-PM-C_{18} group. The black arrows represent inflammatory cells.

The shape and size of particle were the key factors for efficient therapeutic effect of eye disease [35]. FK506-PM-C_{18} with a nano-size around 100 nm is clear and transparent which avoids the problems of blurred vision and discomfort, which further reduce the drug lose through the eye blinks and increase the drug bioavailability. The nano-sized FK506-PM-C_{18} can increase drug permeability and uptake in conjunctival epithelial cells [45] and the bioadhesive drug carrier PM-C_{18} can make FK506 have a longer residence time in conjunctiva [11]. In addition of its sustained release property, compared to FK506 ophthalmic suspension, FK506-PM-C_{18} can reduce the eye instillation times, improve treatment compliance and increase the drug bioavailability.

6. Conclusions

Marine polysaccharide-based nanomaterial as drug delivery system brings undoubted advantages such as non-toxicity, biocompatibility and biodegradability. PM-C_{18} micelle solution was nontoxic, neural, spherical with a narrow particle size range around 110.34 ± 1.6 nm (PDI = 0.236 ± 0.01). FK506-PM-C_{18} had a long lasting release behavior in vitro. The slit lamp evaluation scoring showed us the relieved symptoms of AC. The histological analysis result showed us the decreasing of the inflammatory cells and the improvement of conjunctival tissue. Twice daily FK506-PM-C_{18} eye installation has almost the same effect with three times daily FK506 eye installation which indicated that FK506-PM-C_{18} could ameliorate the ophthalmologic agent and serve as a potential ophthalmic drug for patients with AC. Furthermore, marine polysaccharide polymannuronic acid derivative PM-C_{18} as a biocompatible and biodegradable drug carrier has potential and facile use in the near future.

Funding

This work was financially supported by National Natural Science Foundation of China (31500806), Innovation Project of Qingdao National Laboratory for Marine Science and Technology (No. 2015ASKJ02), Shandong key scientific and technology program (2015ZDJS04002); the Fundamental Research Funds for the Central Universities (201413066) and China Postdoctoral Science Foundation funded project (2014M561969, 2015T80978), NSFC-Shandong Joint Fund (U1406403); Shandong Provincial Natural Science Foundation, China (No. ZR2014YL035), Technology Foundation for Selected Overseas Chinese Scholar of 2014, Ministry of Personnel of China.

Conflicts of interest

We confirm that there is no conflict of interest for our manuscript.

References

[1] P. Manivasagan, J. Oh, Marine polysaccharide-based nanomaterials as a novel source of nanobiotechnological applications, Int. J. Biol. Macromol. 82 (2016) 315–327.
[2] C. Zhang, W. Wang, T. Liu, Y. Wu, H. Guo, P. Wang, Q. Tian, Y. Wang, Z. Yuan, Doxorubicin-loaded glycyrrhetinic acid-modified alginate nanoparticles for liver tumor chemotherapy, Biomaterials 33 (2012) 2187–2196.
[3] R. Jayakumar, M. Prabaharan, S.V. Nair, H. Tamura, Novel chitin and chitosan nanofibers in biomedical applications, Biotechnol. Adv. 28 (2010) 142–150.
[4] S. Raveendran, Y. Yoshida, T. Maekawa, D.S. Kumar, Pharmaceutically versatile sulfated polysaccharide based bionano platforms, Nanomed. Nanotechnol. 9 (2013) 605–626.
[5] R. Gupta, J. Shea, C. Scafe, A. Shurlygina, N. Rapoport, Polymeric micelles and nanoemulsions as drug carriers: therapeutic efficacy, toxicity, and drug resistance, J. Control. Release 212 (2015) 70–77.
[6] U. Kedar, P. Phutane, S. Shidhaye, V. Kadam, Advances in polymeric micelles for drug delivery and tumor targeting, Nanomed. Nanotechnol. 6 (2010) 714–729.
[7] C. Jiang, H. Wang, X. Zhang, Z. Sun, F. Wang, J. Cheng, H. Xie, B. Yu, L. Zhou, Deoxycholic acid-modified chitooligosaccharide/mPEG-PDLLA mixed micelles loaded with paclitaxel for enhanced antitumor efficacy, Int. J. Pharm. 475 (2014) 60–68.
[8] H. Wang, H. Xie, J. Wu, X. Wei, L. Zhou, X. Xu, S. Zheng, Structure-Based rational design of prodrugs to enable their combination with polymeric nanoparticle delivery platforms for enhanced antitumor efficacy, Angew. Chem. Int. Edit. 53 (2014) 11532–11537.
[9] F. Bande, S.S. Arshad, M.H. Bejo, S.A. Kamba, A.R. Omar, Synthesis and characterization of chitosan-Saponin nanoparticle for application in plasmid DNA delivery, J. Nanomater. 16 (2015) 207.
[10] L. Zhao, G. Yang, Y. Shi, C. Su, J. Chang, Co-delivery of Gefitinib and chloroquine by chitosan nanoparticles for overcoming the drug acquired resistance, J. Nanobiotechnol. 13 (2015) 1.
[11] B. Mahaling, D.S. Katti, Understanding the influence of surface properties of nanoparticles and penetration enhancers for improving bioavailability in eye tissues in vivo, Int. J. Pharm. 501 (2016) 1–9.
[12] P. Baranowski, B. Karolewicz, M. Gajda, J. Pluta, Ophthalmic drug dosage forms: characterisation and research methods, The Sci. World J. (2014).
[13] E. Ruvinov, I. Freeman, R. Fredo, S. Cohen, Spontaneous co-assembly of biologically active nanoparticles via affinity binding of heparin-binding proteins to alginate-sulfate, Nano Lett. 16 (2016) 883–888.
[14] B. Yao, C. Ni, C. Xiong, C. Zhu, B. Huang, Hydrophobic modification of sodium alginate and its application in drug controlled release, Bioproc. Biosyst Eng. 33 (2010) 457–463.
[15] A.H. Najafabadi, S. Azodi-Deilami, M. Abdouss, H. Payravand, S. Farzaneh, Synthesis and evaluation of hydroponically alginate nanoparticles as novel carrier for intravenous delivery of propofol, J. Mater. Sci. Mater. M. 26 (2015) 1–11.
[16] R. Kojima, T. Yoshida, H. Tasaki, H. Umejima, M. Maeda, Y. Higashi, S. Watanabe, N. Oku, Release mechanisms of tacrolimus-loaded PLGA and PLA microspheres and immunosuppressive effects of the microspheres in a rat heart transplantation model, Int. J. Pharm. 492 (2015) 20–27.
[17] S. Reitamo, M. Rustin, T. Ruzicka, F. Cambazard, K. Kalimo, P.S. Friedmann, W. Schoepf, F. Lahfa, T.L. Diepgen, H. Judodihardjo, A. Wollenberg, J.J. Berth, T. Bieber, Efficacy and safety of tacrolimus ointment compared with that of hydrocortisone butyrate ointment in adult patients with atopic dermatitis, J. Allergy Clin. Immun. 109 (2002) 547–555.
[18] K. Ikeya, K. Sugimoto, S. Kawasaki, T. Iida, Y. Maruyama, F. Watanabe, H. Hanai, Tacrolimus for remission induction in ulcerative colitis: mayo endoscopic subscore 0 and 1 predict long-term prognosis, Digest. Liver Dis. 47 (2015) 365–371.
[19] N. Ebihara, Y. Ohashi, H. Fujishima, A. Fukushima, Y. Nakagawa, K. Namba, S. Okamoto, J. Shoji, E. Takamura, E. Ochio, D. Miyazaki, Blood level of tacrolimus in patients with severe allergic conjunctivitis treated by 0.1% tacrolimus ophthalmic suspension, Allergol. Int. 61 (2012) 275–282.
[20] A.K. Bakrania, S.S. Patel, Combination treatment for allergic conjunctivitis-Plant derived histidine decarboxylase inhibitor and H1 antihistaminic drug, Exp. Eye Res. 137 (2015) 32–38.
[21] S.J. Ono, M.B. Abelson, Allergic conjunctivitis: update on pathophysiology and prospects for future treatment, J. Allergy Clin. Immun. 115 (2005) 118–122.
[22] Y. Ohashi, N. Ebihara, H. Fujishima, A. Fukushima, N. Kumagai, Y. Nakagawa, K. Namba, S. Okamoto, J. Shoji, E. Takamura, K. Hayashi, A randomized, placebo-controlled clinical trial of tacrolimus ophthalmic suspension 0.1% in severe allergic conjunctivitis, J. Ocul. Pharmacol. Th. 26 (2010) 165–174.
[23] C. Wang, C. Long, C. Xie, X. Chen, L. Zhang, B. Chu, Y. Wang, F. Luo, Z. Qian, Two novel nanoscale preparations of micelle and thermosensitive hydrogel for docetaxel to treat malignant tumor, J. Biomed. Nanotechnol. 9 (2013) 357–366.
[24] C. Gong, S. Deng, Q. Wu, M. Xiang, X. Wei, L. Li, X. Gao, B. Wang, L. Sun, Y. Chen, Y. Li, L. Liu, Z. Qian, Y. Wei, Improving antiangiogenesis and anti-tumor activity of curcumin by biodegradable polymeric micelles, Biomaterials 34 (2013) 1413–1432.
[25] B. Zhuang, L. Du, H. Xu, X. Xu, C. Wang, Y. Fan, M. Cong, J. Yin, H. Li, H. Guan, Self-assembled micelle loading cabazitaxel for therapy of lung cancer, Int. J. Pharm. 499 (2016) 146–155.
[26] Z.G. Gao, H.D. Fain, N. Rapoport, Controlled and targeted tumor chemotherapy by micellar-encapsulated drug and ultrasound, J. Control. Release 102 (2005) 203–222.
[27] G. Kwon, M. Naito, M. Yokoyama, T. Okano, Y. Sakurai, K. Kataoka, Block copolymer micelles for drug delivery: loading and release of doxorubicin, J. Control. Release 48 (1997) 195–201.
[28] K. Kataoka, T. Matsumoto, M. Yokoyama, T. Okano, Y. Sakurai, S. Fukushima, K. Okamoto, G.S. Kwon, Doxorubicin-loaded poly (ethylene glycol)-poly (β-benzyl-l-aspartate) copolymer micelles: their pharmaceutical characteristics and biological significance, J. Control. Release 64 (2000) 143–153.
[29] L. Zhu, Q. Li, F.L. Gong, X.F. Yan, X.Q. Li, G.H. Ma, Z.G. Su, Q.P. Yuan, An insight into structure regulation of uniform polystyrene micro/nano-particles by porogen in premix membrane emulsification process, J. Membrane Sci. 448 (2013) 248–255.
[30] H.J. Byeon, C. Lee, S. Lee, E.S. Lee, H.G. Choi, E.S. Park, Y.S. Youn, Pharmaceutical potential of tacrolimus-loaded albumin nanoparticles having targetability to rheumatoid arthritis tissues, Int. J. Pharm. 497 (2016) 268–276.
[31] D. Liu, Z. Liu, L. Wang, C. Zhang, N. Zhang, Nanostructured lipid carriers as novel carrier for parenteral delivery of docetaxel, Colloids Surfaces B 85 (2011) 262–269.
[32] A.D. Gimenes, T.R.M. Andrade, C.B. Mello, L. Ramos, C.D. Gil, S.M. Oliani, Beneficial effect of annexin A1 in a model of experimental allergic conjunctivitis, Exp. Eye Res. 134 (2015) 24–32.
[33] S.H. Chung, S.Y. Chang, H.J. Lee, S.H. Choi, The CC chemokine receptor 6 (CCR6) is crucial for Th2-driven allergic conjunctivitis, Clin. Immunol. 161 (2015) 110–119.
[34] J. Merayo-Lloves, T.Z. Zhao, J.E. Dutt, C.S. Foster, A new murine model of allergic conjunctivitis and effectiveness of nedocromil sodium, J. Allergy Clin. Immun. 97 (1996) 1129–1140.
[35] Y.F. Fan, B. Zhuang, C. Wang, X. Xu, W. Xu, Z. Lv, Pimecrolimus micelle exhibits excellent therapeutic effect for Keratoconjunctivitis Sicca, Colloids Surfaces B 140 (2016) 1–10.

[36] Xiuqiong Chen, et al., Synthesis of amphiphilic alginate derivatives and electrospinning blend nanofibers: a novel hydrophobic drug carrier, Polym. Bull. 72 (2015) 3097–3117.
[37] S.M. Moghimi, J. Szebeni, Stealth liposomes and long circulating nanoparticles: critical issues in pharmacokinetics, opsonization and protein-binding properties, Prog. Lipid Res. 42 (2003) 463–478.
[38] V.P. Torchilin, Micellar nanocarriers: pharmaceutical perspectives, Pharm. Res. 24 (2007) 1–16.
[39] K.Y. Win, S.S. Feng, Effects of particle size and surface coating on cellular uptake of polymeric nanoparticles for oral delivery of anticancer drugs, Biomaterials 26 (2005) 2713–2722.
[40] J.F. Hillyer, R.M. Albrecht, Gastrointestinal persorption and tissue distribution of differently sized colloidal gold nanoparticles, J. Pharm. Sci-us. 90 (2001) 1927–1936.
[41] S. Dash, P.N. Murthy, L. Nath, P. Chowdhury, Kinetic modeling on drug release from controlled drug delivery systems, Acta. Pol. Pharm. 67 (2010) 217–223.
[42] Q. Gan, T. Wang, Chitosan nanoparticle as protein delivery carrier—systematic examination of fabrication conditions for efficient loading and release, Colloids Surfaces B 59 (2007) 24–34.
[43] W. Su, Q. Wan, J. Huang, L. Han, X. Chen, G. Chen, N. Olsen, S.G. Zheng, D. Liang, Culture medium from TNF-α-stimulated mesenchymal stem cells attenuates allergic conjunctivitis through multiple antiallergic mechanisms, J. Allergy Clin. Immun. 136 (2015) 423–432.
[44] M.J. Doughty, Goblet cells of the normal human bulbar conjunctiva and their assessment by impression cytology sampling, Ocul. Surf. 10 (2012) 149–169.
[45] M.G. Qaddoumi, H. Ueda, J. Yang, J. Davda, V. Labhasetwar, V.H. Lee, The characteristics and mechanisms of uptake of PLGA nanoparticles in rabbit conjunctival epithelial cell layers, Pharm. Res. 21 (2004) 641–648.